Molecular isomerization induced by ultrashort infrared pulses. I. Few-cycle to sub-one-cycle gaussian pulses and the role of the carrier-envelope phase

Christoph Uiberacker* and Werner Jakubetz†

Institut für theoretische Chemie und Molekulare Strukturbiologie, Universität Wien, Währinger Str. 17, A-1090 Wien, Austria

(Dated: March 16, 2004)

Abstract

Using 550 previously calculated vibrational energy levels and dipole moments we performed simulations of the HCN→HNC isomerization dynamics induced by sub-one-cycle and few-cycle ir pulses, which we represent as gaussian pulses with 0.25 to 2 optical cycles in the pulse width. Starting from vibrationally pre-excited states, isomerization probabilities of up to 50% are obtained for optimized pulses. With decreasing number of optical cycles a strong dependence on the carrier-envelope phase (CEP) emerges. Although the optimized pulse parameters change significantly with the number of optical cycles, the distortion by the gaussian envelope produces nearly equal fields, with a positive lobe followed by a negative one. The positions and areas of the lobes are also almost unchanged, irrespective of the number of cycles in the halfwidth. Isomerization proceeds via a pump-dump-like mechanism induced by the sequential lobes. The first lobe prepares a wavepacket incorporating many delocalized states above the barrier. It is the motion of this wavepacket across the barrier, which determines the timing of the pump- and dump lobes. The role of the pulse parameters, and in particular of the CEP, is to produce the correct lobe sequence, size and timing within a continuous pulse.

*Electronic address: christoph.uiberacker@univie.ac.at

†Electronic address: werner.jakubetz@univie.ac.at

I. INTRODUCTION

Over the last few years there has been considerable progress in generating and employing ultrashort few-cycle laser pulses [1], down to half-cycle pulses. Theoretical work and numerical simulations have accompanied these developments [2]. Compared with traditional (many-cycle) laser pulses, due to the much broader Fourier spectrum the importance of the central frequency diminishes and begins to lose its meaning as the number of cycles is decreased, while the carrier envelope phase (CEP) [3] becomes a decisive parameter.

Few-cycle and half-cycle pulses in the infrared (ir) regime may provide interesting possibilities for inducing and controling molecular systems. Pioneering work in the field of the dynamics of photochemical processes using such pulses has been reported by Korolkov et al. [4], who investigated the dynamics of dissociation via stretch vibration of the OH bond in H_2O and HOD. They found that a strong dependence of the dissociation probability on the CEP emerges for pulses with only a few cycles, which shows a 2π periodicity. Furthermore, if a certain CEP gives rise to strong dissociation, then the same phase with π added gives the smallest effect, implying there is a marked dependence on the sign of the field. Korolkov et. al. found that for those values of the CEP where the dissociation probability is smallest, the dynamics induced by half-cycle pulses can be understood as a continuous pump-dump process to high-lying vibrational states via continuum states, which may occur within a single half-cycle of a field. It is the de-excitation by the dump which leads to the somewhat unexpected arrest of dissociation.

In the present paper we take up these findings and apply the same concepts to systems characterized by double-well potentials. In such systems, a continuous pump-dump mechanism may allow population transfer across a barrier from a state localized in the potential well corresponding to one of the isomers to states localized in the other well. Due to the broad frequency spectrum of few-cycle pulses such a mechanism may be viable even if the transition frequencies in the two wells are markedly different. In particular we deal with the problem of molecular isomerization in a single electronic state [5] induced by ultrashort half-, one- or few-cycle pulses. The initial and final isomers correspond to different wells on the multi-dimensional potential surface, which are separated by the isomerization barrier.

As our specific model system, we have chosen the HCN→HNC isomerization, which has become a prototype system for the simulation of laser-controled isomerization reactions [6–

10]. However, due to the formal similarity of the respective Hamiltonians our analysis should also apply to other reactions involving vibrationally excited states, and more generally to other problems involving barrier crossing in double well potentials. Indeed the spirit of our investigation is that of a model treatment: we put our emphasis on the principles of the action of few-cycle pulses in double-well systems and on the response of the dynamical behavior to variations of the laser- and system-parameters. We largely put aside practical issues like the consideration of the ionization barrier (Keldysh limit [11]) or the laboratory availability of the pulses, noting however that these points could be discussed on the basis of our results.

In Section II below we present our model system, and we give a brief account of the theoretical and computational background of our simulations. Our main results are collected and discussed in Section III. In particular we focus on the transfer mechanisms involved and on other "generic" features arising independent of specific pulse parametrizations. Finally, a summary and conclusions are presented in Section IV.

In a companion paper, [12] we give a comprehensive discussion of the dynamics in terms of wavepacket propagation, and we extend the simulations to a pump-dump setup with pairs of time-delayed single-lobe half-cycle pulses.

II. THEORETICAL AND COMPUTATIONAL ASPECTS

A. The Hamiltonian

The molecular Hamiltonian of the HCN/HNC system has been described in detail in previous papers.[6, 10] In brief, the potential energy surface and vibrational wave functions are taken from the calculations of Bowman et. al. [13]. In the calculations reported in the present paper, the lowest 550 $J = 0$ vibrational states have been selected, and we verified the convergence of our results for selected cases by using a basis of 750 states.

We focus on ultrashort few-cycle and sub-one cycle pulses, down to single lobes. This regime is hard to analyse by either model calculations or analytical theory, because it differs from the usual case in a number of points. The envelope function varies strongly over one optical cycle so that one cannot average the contribution of the electric field to the diagonal part of the Hamiltonian. The Fourier spectrum is very broad leading to very large detunings.

Furthermore, due to the high field strengths required, multiphoton processes may play an important role. That means that neither adiabatic Floquet theory nor the rotating wave approximation (RWA) can be used and therefore we directly integrate the time-dependent Schrödinger equation.

The semiclassical dipole approximation has been used to describe the interaction of the molecule with the laser field, and rotation has been neglected. Expanding the total wavefunction $\Psi(t)$ in the basis of vibrational eigenfunctions, the Hamiltonian can be written in algebraic form, and the time-dependent Schrödinger equation reads

$$i\dot{c}_{\mathsf{k}} = (\epsilon_{\mathsf{k}} - E(t)\mu_{\mathsf{kk}})c_{\mathsf{k}} - \sum_{\mathsf{l}=1}^{N_{\mathsf{B}}} E(t)\mu_{\mathsf{kl}}c_{\mathsf{l}}, \quad k = 1, ..., N_{\mathsf{B}}\,. \tag{1}$$

The c_{k} are the time dependent expansion coefficients of $\Psi(t)$, N_{B} is the size of the basis set (i.e. $N_{\mathsf{B}} = 550$ in the bulk of our calculations), the ϵ_{k} are the vibrational eigenvalues, and the μ_{kl} are the dipole matrix elements, which were calculated using the dipole moment surface of Jakubetz and Lan.[6] Finally, $E(t)$ is the scalar field strength corresponding to one laser pulse with Gaussian envelope assumed to be linearly polarized in the direction of the C-N bond, and is given by

$$E(t) = A \exp\left[-\frac{ln2}{(\alpha)^2}\left(t - \frac{\tau}{2}\right)^2\right] \cos[\omega(t - \frac{\tau}{2}) + \phi] \quad . \tag{2}$$

Here A is the amplitude, ω is the frequency, related to the optical cycle T by $\omega := 2\pi/T$, α is the halfwidth of the pulse at half maximum (HWHM), and the phase ϕ is the CEP. The maximum of the envelope occurs at $\tau/2$. Our integration interval extends from $t = 0$ to $t = \tau$ and we set $\tau = 6.67\alpha$, which guarantees that the field is effectively zero at the beginning and the end of the integration.

Except for the time we use atomic units (au), with the conversion factors 1 au of energy = 1 hartree = 2625.57 kJ mol^{-1} (numerically equal to 1 au of frequency), and 1 au of field strength = 1 hartree $q_{\mathsf{e}}^{-1}a_0^{-1} = 5.14225$ GV cm^{-1}.

B. Construction of sub-one cycle- and few-cycle pulses

In order to have a well-defined prescription for the construction of few-cycle pulses with continuously variable CEP, we specify n_{c} as the number of optical cycles in the width

(FWHH) of the envelope. More precisely, for a given n_c α is adjusted to T so that

$$2\alpha = n_c T \quad , \tag{3}$$

using $n_c = 0.25$, 0.5, 1 or 2. Note this links the pulse length to the central frequency. For notational convenience we will refer to these pulses as "gaussian 0.25-, 0.5-, 1-cycle and 2-cycle pulses", noting that additional, more or less strongly damped oscillations are present in the wings of the pulses. Figures 1 and 2 illustrate the construction and properties of the limiting cases of such pulses, i.e. $\phi = 0$ (cosine-pulse) and $\phi = \pi/2$ ($-$sine pulse). For $n = 0.25$ the additional oscillations mentioned above are vanishingly small, so that the gaussian 0.25-cyle pulses closely correspond to the idealized picture of half-cycle pulses: it has just one lobe. On the other hand, gaussian 0.25- and 0.5-cycle sine-pulses resemble one-cycle pulses with an effective optical cycle length (or frequency) drastically different from the nominal value in the cosine part of eq. 2.

For $n_c < 1$, corresponding cosine- and sine- pulses have different effective maximum field strengths, and thus different intensities. Cosine- and sine pulses also have markedly different Fourier spectra, while such CEP-related differences disappear for the 1- and 2- cycle gaussian pulses. Yet for all pulse types considered the width of the frequency distribution is large enough to cover both the HCN- and HNC bend progressions ($\omega_{\mathrm{HCN}} \approx 1.5\omega_{\mathrm{HNC}}$) as well as all anharmonicity effects. The sub-one- cycle cosine pulses also have very low-frequency parts and a dc component, which however do not contribute to the dynamics of isomerization.

In order to separate trivial intensity-dependent effects from the interesting dynamical ones, in those sets of calculations where different pulses are compared, A was scaled with the remaining parameters so as to keep the fluence F, given by

$$\begin{aligned} F &:= \int_{-\infty}^{\infty} \mathrm{d}t E(t)^2 \\ &= \frac{A^2 n_c \pi}{2\omega} \sqrt{\frac{\pi}{2\ln(2)}} \left(1 + \exp(-\frac{\pi^2 n_c{}^2}{2\ln(2)}) \cos(2\phi)\right) \quad , \end{aligned} \tag{4}$$

constant. This makes the intensities of the laser fields equal within a set of simulations.

For gaussian pulses this scaling results in A depending on n_c, ω and ϕ,

$$A(n_c, T, \phi) = A_0 \sqrt{\frac{n_{c;0} T_0}{n_c T} \frac{1 + \exp(-\frac{\pi^2 n_{c;0}^2}{2\ln(2)}) \cos(2\phi_0)}{1 + \exp(-\frac{\pi^2 n_c^2}{2\ln(2)}) \cos(2\phi)}} \quad , \tag{5}$$

where A_0, T_0, $n_{\mathtt{c};0}$ and ϕ_0 are a set of reference values. Since the exponential in the denominator of eq. 5 scales with $-n_{\mathtt{c}}^2$ it follows that the dependence on ϕ_0 is noticable only for $n_{\mathtt{c}}$ well below 1, so that 0.25-cycle or 0.5-cycle gaussian cosine-pulses have a distinctly larger fluence than sine-pulses with otherwise equal parameters.

C. Initial and final states

HCN isomerization proceeds most efficiently along the bend progressions of HCN and HNC [6], i.e. the states labeled $(0, v_2, 0)$. While bend vibrational excitation of HCN out of the ground state $(0, 0, 0)$ is best achieved by a pulse polarized perpendicular to this axis, barrier crossing is most efficiently induced by a pulse polarized along the CN axis [7]. Since our main interest is the passage of the system over the barrier, we focus on isomerization starting from a vibrationally excited state, disregarding the vibrational excitation of the molecule from the HCN ground state and assuming that the molecule has been promoted to its excited initial state by some other appropriate means. We select one of the pure bend states $(0, v_2, 0)$, where v_2 is even in the $J = 0$ manifold. In addition to bend states we have also investigated several stretch excited states as the initial state, but with much less success.

Our target are all states below the isomerization barrier, which are localized in the potential well corresponding to the HNC isomer. Throughout this paper we refer to this group of 62 states as "HNC". Furthermore, we denote the sum of population in these states as "total HNC population" (P_{HNC}), noting that additional HNC population may reside in localized HNC states above the isomerization barrier, as well as in delocalized states. In order to analyse the dynamics of the isomerization more compactly, we consider the populations in several additional groups of states. In analogy to HNC, the 121 states below the barrier localized in the HCN well are denoted as "HCN" states, with population P_{HCN}. These states are further partitioned into the "initial" state (P_{init}), the states "HCN$_<$" below the initial state, with group population $P_<$, and "HCN$_>$" above the initial state ($P_>$). In our basis of 550 states, the 367 states above the barrier comprise 156 localized HCN states, 107 localized HNC states, and 124 delocalized states with at least 5% of the total density in each of the HCN or HNC "hemispheres" of configuration space. It turns out that only the delocalized states become appreciably populated. We denote this group as "delocalized"

and the corresponding group population as $P_{\rm del}$.

III. RESULTS AND DISCUSSION

A. Isomerization probabilities

With optimized pulse parameters, isomerization in the HCN→HNC model system from pre-excited vibrational states can be induced by gaussian sub-one-cycle and few- cycle pulses, with isomerization probabilities approaching 50%. The results are quite stable both against variation of $n_{\mathbf{c}}$, and also against variation of the initial state, provided only it is taken from the bend state manifold.

The effect of the variation of the initial state is illustrated in Figure 3. Here we plot the A-dependence of the maximum isomerization probability, when $n_{\mathbf{c}}$ is set to 0.5, taking in turn each of the bend states as initial state. For each point on the curves A is fixed, whereas the remaining pulse parameters are adjusted to give the maximum $P_{\rm HNC}$. The similarity of the qualitative features of the plots is striking, and even quantitatively the differences remain small, except for the expected shift in the required field strength. The similarity extends to other observables, and indeed to the full dynamics of the process.

Hence it suffices to restrict the detailed investigation of the isomerization to one arbitrarily chosen initial state. The bulk of our results reported below has been obtained with $(0, 16, 0)$ as initial state. This state is connected to the lowest delocalized states by a 4-quantum transition along the HCN-bend ladder. With this choice, a maximum $P_{\rm HNC}$ of about 0.45 can be obtained upon full optimization of the pulse parameters.

As already noted, this result is also fairly independent of $n_{\mathbf{c}}$. We first consider the case of gaussian 0.25-cycle pulses. In Figure 4 we show $P_{\rm HNC}$ as a function of T and ϕ (over the range 0 to 2π) for various fixed amplitudes A. We notice the strong initial increase of $P_{\rm HNC}$ with A already seen in Figure 3. Saturation occurs at a value of ≈ 0.42. For all amplitudes, $P_{\rm HNC}$ is single peaked, and the peak is fairly broad in the direction of T, but extremely narrow, almost razor-edge like, in the direction of ϕ. This indicates a strong sensitivity of the isomerization to the CEP. The value of ϕ associated with the constrained maximum of $P_{\rm HNC}$ increases very weakly with A. When $P_{\rm HNC}$ has its global maximum, its value is $\approx 0.52\pi$, roughly corresponding to a $-$sine-pulse in a re-formulation of eq. 2 Away from the

peak, P_{HNC} is effectively zero, the minimum occuring at $\phi_{\max} + \pi$. The 2π-periodicity with respect to ϕ implies that the dynamics crucially depend on the sign of the laser field.

The insensitivity of P_{HNC} with respect to T is consistent with the large extension of the Fourier spectra in Figure 1. However, the maximum, which extends from about $T = 94$ fs to more than 100 fs, is very strongly red-shifted with respect to the bend level spacings of either HCN (≈30 fs) or HNC (≈ 45 fs). For a frequency-driven process encompassing both HCN- and HNC bend transitions one would expect a value near the harmonic mean of the spacings, i.e. near T =35 fs. In section II.C we have already noted that the physical meaning of the pulse parameters begins to disappear for $n_{\mathsf{c}} \leq 1$. The observed shift in T is expected in view of the strong change of the effective optical cycle-length of sine-like gaussian sub-one-cycle pulses.

In Figure 5, we collect plots analogous to those in Figure 4, comparing now the optimized pulses for $n_{\mathsf{c}} = 0.25$ to 2. The results for maximum isomerization at the onset of saturation are shown. The examples share most of the overall features seen for $n_{\mathsf{c}} = 0.25$. For $n = 2$ the maximum P_{HNC} is slightly larger (≈ 0.45), and three general trends accompany the transition from $n_{\mathsf{c}} = 0.25$ to $n_{\mathsf{c}} = 2$. The peak in P_{HNC} moves towards the expected T-range between ≈ 30 and 45 au, gets somewhat sharper in the direction of T, and gets broader in the direction of ϕ. Indeed, for the gaussian 2-cycle pulses we observe the beginning disappearence of the CEP- dependence: while there still is a distinct single maximum, the peak now almost extends over the full CEP range from 0 to 2π.

Summarizing these observations, it can be stated that the overall properties of the isomerization appear unchanged upon going from gaussian 2-cycle to 0.25-cycle pulses, but this superficial insensitivity of the net result is accompanied by a distinct change in the topography of the probability landscape, which indicates the transition from the usual frequency-controled (multiphoton-) dynamics to a CEP-controled one.

Since the isomerization process seems to possess properties universial to all gaussian pulses we have used, we next attempt to extract the essential parameters of the optimal fields. To this end, in Figure 6a we plot the laser fields for the various optimized gaussian pulses at the onset of saturation. With the time origin adjusted to be at the central zero of the field for each of the pulses, it becomes apparent that despite the sizable differences in the nominal parameters, all these fields approximately coincide in the center of the pulse, and diverge only in the wings. In fact all pulse forms seem to produce roughly the same

effective one-cycle −sine-pulse. The individual lobes may be distorted, but the fluence of the positive central lobe, or of the first part of the pulse up to and including this lobe, are conserved. The following negative lobe has some variability with respect to its size.

Therefore, all pulses achieving high isomerization yields have the following near-invariant properties:

- There is a large positive lobe with an optimum intensity
- It is followed by a large negative lobe with an intensity exceeding a minimum value
- The maximum-to-minimum distance of these lobes is ≈19 fs.

The optimal pulses thus all have a universal effective optical cycle length $T_{\rm eff}$ of ≈38 fs.

This argument is further enhanced by the fact that all other combinations of field lobes satisfying above conditions also induce isomerization with yields around 40%. Thus Figure 6a includes combinations of two simple sine-lobes. The two lobes need not even be continuously connected: narrower lobes (with smaller values of T, but appropriately larger values of A) do the same job.

B. Population dynamics

In order to understand the mechanism of the reaction it is useful to investigate the time-resolved population of various important groups of states as defined in Section II. In Figure 6b we superimpose the population dynamics for the various successful pulses. Additional information can be gained from the time evolution of the system's energy expectation value $< \epsilon >$ and the various group energy expectation values $< \epsilon_{\rm G} >$ in Figure 6c. The latter are defined as

$$< \epsilon_{\rm G} >= \frac{1}{P_{\rm G}} \sum_{\rm I \in G} \epsilon_{\rm I} \quad , \tag{6}$$

where G is any of the groups of states.

The group populations and energy expectation values overlap just the way the fields do, especially $P_{\rm del}$ and $P_{\rm HNC}$. This behaviour supports our assumption that indeed it is only the timing between the lobes that is of importance, while the form of each lobe can be modified without risk of loosing product. The only notable difference arises in $< \epsilon_{\rm HNC} >$. This is due to the fact that the fluence need not be uniform for the second lobe. Beyond a certain

minimum size required for the dump to HNC well states, a more intense second lobe simply drives the population further down the HNC well. This results in the observed decrease of $< \epsilon_{\mathrm{HNC}} >$. There is also a difference concerning the initial depletion of the initial state. For the more- cycle pulses this process starts already with the small field oscillations in the wing of the envelope, induces a pre-excitation to $\mathrm{HCN}_{>}$ states. However, it does not contribute to the population of delocalized states, which is all built up by the central positive lobe.

It is interesting to analyse the population dynamics in more detail and to compare the succesful pulse with cases where no isomerization is induced. In Figures 7a and 8a we show respectively the population dynamics and the evolution of the energy expectation values for the optimized gaussian 0.25-cycle pulse, with T =97 fs, A =0.13 and $\phi = \phi_{\mathrm{opt}} = 0.52\pi$, and contrast it with the unsuccesful cases for the opposite sine-like field, i.e. for $\phi_{\mathrm{opt}} + \pi$ in panels (b), and with the cosine-like fields at $\phi = 0$ and π in panels (c) and (d).

For both sine-like cases, two main steps occur which are separated in time and are associated with the first and the second lobe of the field. At the onset of the pulse, both field directions induce the same behaviour. The initial state is rapidly depleted by simultaneous population transfer to the $\mathrm{HCN}_{<}$ and $\mathrm{HCN}_{>}$ states. The population in the lower states is then effectively trapped and is not available for isomerization. In a typical ladder-climbing process, the population in $\mathrm{HCN}_{>}$ is passed on to the delocalized states above the barrier. At the point of reaching the delocalized states, close to the field maximum or minimum, the two cases begin to diverge. For the successful case at ϕ_{opt}, the excitation to the delocalized states continues, while for the negative lobe the direction of population transfer is reversed back to the HCN states. This sign-dependent behavior is analogous to the internal pump-dump mechanism inhibiting molecular dissociation, as observed by Korolkov et al. [4].

For the $-$sine-case in panel (a), by the end of the first lobe almost all of the excited population is found in the delocalized states, where it is available for dumping to the product HNC states by the subsequent negative lobe. In contrast, for the +sine-case in panel (b) no delocalized state population is available, and the second lobe can only re- excite HCN to the delocalized states. This different behaviour can be clearly discerned by following the energy expectation value $< E >$ of the molecular system, which is shown in Figure 8.

As to the cosine-like single lobed pulses, a +cosine pulse induces dynamics similar to the first (positive) lobe in Figure 7a and the second (positive) lobe in Figure 7b, namely an excitation to delocalized states. The $-$cosine pulse compares to the first (negative) lobe in

Figure 7b. The resulting internal pump-dump process leads to no net excitation. In both cases no HNC product is formed.

The previous discussion makes clear that in a continuous single pulse only a pattern of a positive lobe followed by a negative one can drive the reaction. For gaussian pulses the CEP is therefore of such a value as to guarantee this situation. As a result, for $n_{\mathsf{c}} < 1$ the CEP attains a value very close to $\pi/2$, which together with the damping property of the gaussian envelope produces exactly this pattern. For $n_{\mathsf{c}} = 1$ or 2, the damping decreases compared to the optical cycle. Therefore the CEP looses its role in producing the sinusoidal pattern and only needs to ascertain the correct partitioning of the fluence to the pump- and dump-parts of the pulse.

For $n_{\mathsf{c}} = 2$, the A-dependence of P_{HNC} shows a secondary maximum in the range of saturation, which leads to a weak enhancement of isomerization. Since for $n_{\mathsf{c}} \geq 2$, T becomes small compared to the gaussian width, the oscillations in the wing may become large enough to set up a second round of pump-dump isomerization independent of the first one, adding a small contribution to P_{HNC}. The phase relation which adjusts the timing obviously will be the same as the one for the central pair of lobes.

C. One dimensional reaction path dynamics

Looking at the population dynamics in closer detail, one finds that the dominant contributions to the HCN- and the HNC-states in the well come from the pure bend states, even though within each group these states cover only a small fraction of the available phase space. Similarly, the delocalized states dominate among the high-lying ones, despite occupying only about a third of the phase space. Since these dominant states are spread out along the reaction path, to a first approximation isomerization can be described as a one-dimensional process proceeding along the reaction-coordinate.

We have verified that in a pseudo-one dimensional 50-level system comprising the dominant states of our three-dimensional system, i.e. the $(0, v_2, 0)$ bend states in both wells and the most strongly coupled delocalized states, the results resemble those for the full 550- level system. An even closer matching of the overall results can be obtained by suitable parametrization of a one-dimensional model potential. As an illustration, Figure 9 compares side by side typical results for the present three-dimensional HCN/HNC system and those

obtained for an unsymmetric one-dimensional quartic double-well potential. A detailed discussion of this point, as well as a presentation of the one-dimensional potential will be given in part II.[12]

D. Interpretation in terms of vibrational wavepackets

The extended plateau region in the time-resolved populations separating the excitation to the delocalized states and the de-excitation to the product states suggests a wavepacket interpretation of the dynamics. The more intense parts of the first lobe prepare a vibrational wavepacket containing components of HCN-states and delocalized ones, which then evolves freely until the field becomes sizeable again. If by that time the delocalized portion of the wavepacket has succeeded in crossing the barrier, a dump to the HNC well states may be triggered by the second lobe. It then follows that it is the barrier crossing time of the delocalized part of the wavepacket, which determines the correct spacing between the field lobes. It implicitly fixes the optimal pulse parameters, in particular the optical cycle length.

Relaxing the requirement to perform isomerization with one single pulse, the motion of a wavepacket across the barrier and across both wells suggests the possibility of a pump- dump isomerization using pairs of time-delayed single lobe pulses, as well as the occurence and observation of vibrational recurrences. Furthermore, in view of the quasi- one-dimensional nature of the isomerization mechanism, the analysis and the visualization of the wavepacket dynamics may be carried out in terms of wavepacket motion in a one- dimensional double-minimum potential, to be reported in part II. [12]

IV. SUMMARY AND CONCLUSIONS

We report simulations of population transfer across the barrier in a 3-dimensional double-well system, driven by laser fields consisting of single few-cycle down to sub-one-cycle pulses. The latter are constructed as gaussian pulses with $n_{\mathsf{c}} = 0.25$, 0.5, 1 and 2 optical cycles in the width of the envelope.

We make use of a realistic molecular model system based on ab initio data, namely the HCN→HNC isomerization represented by a 550-level system comprising the lowest $J = 0$ vibrational states. Neglecting rotation and placing the system initially in a vibrationally

excited bend state $(0, v_2, 0)$, upon optimization of the optical cycle T, the phase (CEP) ϕ and the amplitude A of the laser field we obtain population transfer probabilities across the barrier, i.e. isomerization yields of up to 50%, depending only weakly on n_c or v_2.

An increasing sensitivity of the isomerization probability to the CEP is emerging in the few-cycle regime, which becomes extremely pronounced in the regime of sub-one-cycle pulses. For such pulses the transfer probability is zero everywhere in the full period of 2π except near an extremely narrow peak close to $\pi/2$. With increasing number of cycles, the range of appropriate values of the CEP increases, i.e. the more cycles the pulse has, the less relevant becomes its phase. Even though the range of acceptable values of ϕ is already fairly extended for $n_c = 2$, the same interpretation of the dynamics applies for all types of pulses investigated: The largest positive peak of the field induces the pump reaction from the initial state to the delocalized states (above the barrier) via the states in between. The following (largest) negative peak induces the dump process from the delocalized states to the HNC states, which to more than 70% are pure bend states. Smaller field oscillations before this central pair assist the excitation to HCN$_>$ states, but do not induce sizable population transfer.

The deviation of the optimal CEP from $\pi/2$ and hence of the optimal pulse from the pure $-$sine form stems from the fact that different field intensities are needed for the pump (by the first lobe) and the dump (by the second lobe).

In a single continuous pulse, only the pattern positive lobe-negative lobe leads to isomerization. However, the sign of the field will be reversed if the signs of the dipole moments of the isomer states are reversed. The present system goes from a negative dipole moment (for HCN bend states) via $\approx$ zero (for delocalized states) to a positive one (for HNC bend states). It is an essential requirement that along the sequence of states from the initial state via the delocalized states to the product states the dipole moments change monotonically. [14]

Above we have noted that another essential parameter for successful isomerization is the timing between the peaks, which determines the effective cycle length of the pulse. The isomerization is clearly less sensitive to variations in the timing than it is to variations in the CEP, as is evident from the considerable extension of the peak in P_{HNC} in direction of T. We find that a variation in the effective cycle length of $\pm$ 10% leads to a relative decrease in P_{HNC} of about 3%.

The mechanism of the laser-induced isomerization with few- or effective one-cycle pulses can be understood as a pump-dump process, with the pump triggered by the first lobe of the pulse, an essentially one-dimensional wavepacket dynamics involving delocalized states, which effects the well-to-well transfer, and the dump by the second lobe. This is discussed in a companion article.[12] In addition, analytical results regarding such reactions in laser fields by using strong-field techniques are in preparation.[14]

This mechanism is robust in several respects. First, it is not very sensitive to pulse parameters other than the CEP. Second, it is only mildly sensitive to the timing of the pulse (steered by pulse length, optical cycle or carrier frequency). Third, near the optimum the transfer probability is quite insensitive to the pulse amplitude, which can be varied almost freely when it is in its range of saturation. Fourth, the exact form of the lobes is irrelevant as long as a scaling law for the intensity of the first (pump-) lobe is observed. In a semi-quantitative way the mechanism is also robust to variations of the initial state, as long as this is a bend state, and robust even against changes in the system. With appropriate scaling our findings should be relevant for other isomerization reactions, and indeed for other types of population transfer in double-well systems.

Acknowledgments

This work was sponsored by the Austrian Science Fund within the framework of the Special Research Program F016 "ADLIS".

[1] T. Brabec and F. Krausz, Rev. Mod. Phys. **72**, 55 (2000).

[2] C. Lemell, X.-M. Tong, F. Krausz, and J. Burgdörfer, Phys. Rev. Lett. **90**, 076403-1 (2003).

[3] R. Kienberger, M. Hentschel, M. Uiberacker, Ch. Spielmann, M. Kitzler, A. Scrinzi, M. Wieland, Th. Westerwalbesloh, U.Kleineberg, U. Heinzmann, M. Drescher, and F. Krausz, Science **297**, 1144 (2002).

[4] M. V. Korolkov, J. Manz, and G. K. Paramonov, Chem. Phys. **217**, 341 (1997).

[5] N. Doslić, Y. Fujimura, L. González, K. Hoki, O. Kühn, J. Manz, and Y. Ohtsuki, in Femtochemistry, edited by F. C. De Schryver, S. De Feyter, and G. Schweitzer (Wiley-VCH, Weinheim, 2001), p. 189.

[6] W. Jakubetz and B. L. Lan, Chem. Phys. **217**, 375 (1997); W. Jakubetz, Faraday Discuss. **113**, 355 (1999).

[7] S. Chelkowski and A. D. Bandrauk, Chem. Phys. Lett. **233**, 185 (1995).

[8] S. P. Shah and S. A. Rice, Faraday Discuss. **113**, 113/15 (1999); S. P. Shah and S. A. Rice, J. Chem. Phys. **113**, 6536 (2000).

[9] V. Kurkal and S. A. Rice, Chem. Phys. Lett. **344**, 125 (2001).

[10] I. Vrábel and W. Jakubetz, J. Chem. Phys **118**, 7366 (2003).

[11] P. Dietrich and P. Corkum, J. Chem. Phys. **97**, 3187 (1992); L. V. Keldysh, Soviet Physics JETP **20**, 1307, (1965).

[12] C. Uiberacker and W. Jakubetz, part II, following article.

[13] J. M. Bowman, B. Gazdy, J. A. Bentley, T. J. Lee, and C. E. Dateo, J. Chem. Phys. **99**, 308 (1993).

[14] C. Uiberacker and W. Jakubetz, to be published.

Figure captions

Figure 1. The construction of a gaussian pulse with $n_c = 0.25$. Left panels: one half-cycle of the carrier oscillation term superimposed on twice the full width at half height of the gaussian envelope. Right panels: The resulting electric fields. Upper panels: CEP set to $\pi/2$, resulting in an effective one-cycle $-$sine-pulse. Lower panels: CEP set to 0, resulting in an effective half-cycle cosine-pulse. The time origin is set to the peak of the envelope, and abscissa scales are in reduced units.

Figure 2. Electric fields and Fourier spectra of gaussian few- and sub-one-cycle pulses. Left panels: Gaussian pulses with $n_c = 0.25$ (full lines), 0.5 (dashed), 1 (short dashed), and 2 (thin full lines). Right panels: The corresponding Fourier spectra. The CEP is adjusted to $\pi/2$ ($-$sine pulses) in the upper panels and to 0 (cosine pulses) in the lower panels. The time origin is set to the peak of the envelope, and abscissa scales are in reduced units.

Figure 3. A-depencence of isomerization probabilities P_{HNC} for different initial states $(0, v_2, 0)$, with $v_2 = 0, 2, \ldots, 20$. The bold line denotes the initial state (0,16,0), which was used in the detailed analysis. The short-dashed vertical line is an estimate for the Keldysh limit.

Figure 4. Isomerization probability landscapes. P_{HNC} against optical cycle T and CEP ϕ for gaussian pulses with $n_c = 0.25$ and different values of A_0. Panels (a) $A = 0.0212$ au; (b) $A = 0.0245$ au; (c) $A = 0.0300$ au (onset of saturation); (d) $A = 0.0367$ au (post-saturation). The initial state is (0,16,0). Within each plot, the values of A are scaled for constant fluence (see text).

Figure 5. Isomerization probability landscapes. P_{HNC} against optical cycle T and CEP ϕ for various optimized gaussian pulses with A at the onset of saturation. Panels (a) $n_c = 0.25$; (b) $n_c = 0.5$; (c) $n_c = 1$; (d) $n_c = 2a$. Within each plot, the values of A are scaled for constant fluence (see text). Note the change in scale and range of the optical cycle upon going from panel (a) to panel (b).

Figure 6. Near-invariance of optimized fields and the corresponding population dynamics. Panel (a): Juxtaposition of optimized (effective one-cycle) gaussian pulses with $n_c = 0.25$

(full line), 0.50 (dashed), and 1 (short dashed), and separate sinusoidal half-cycle lobes of different cycle lengths (dotted and dash-dotted). Panels (b) and (c): Corresponding time resolved populations for important groups of states P_{group} as indicated. Panel (d): Corresponding time evolution of the energy expectation values ϵ_{G} of the delocalized and HNC states. For all curves the time origin is set to the central zero of the field.

Figure 7. Time resolved population of relevant groups of states for pulses with $n_{\mathsf{c}} = 0.25$ and A =0.125 au: Initial state (thin full lines), product HNC (extra-bold full line), delocalized states (bold full line), $\mathrm{HCN}_{<}$ (dashed), and $\mathrm{HCN}_{>}$ (short dashed). Panel (a)-(d) show in turn the optimized pulse at a CEP $\phi = 0.495\pi$ $(-\pi/2)$, and pulses with $\phi = 0.995\pi$, $\phi = 0$, and $\phi = \pi$. The corresponding fields are included offset and scaled for better visibility.

Figure 8. Time evolution of the energy expectation value $< \epsilon >$ (full lines). Panels (a) to (d) correspond to those in Figure 7. The fields shown as dashed line inserts.

Figure 9. Comparison of optimized fields (n_{c} =0.5) and the corresponding population dynamics for the three-dimensional HCN/HNC system (left panels) and a one-dimensional quartic double-well potential (right panels). Plot conventions are as in Figure 7.

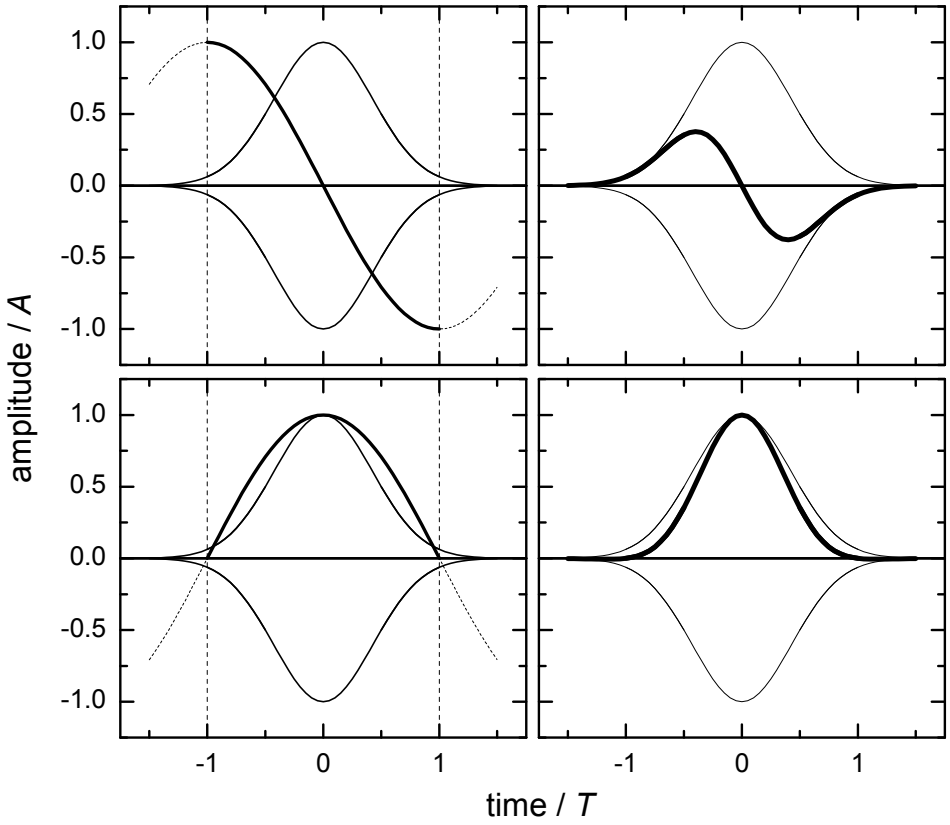

FIG. 1:

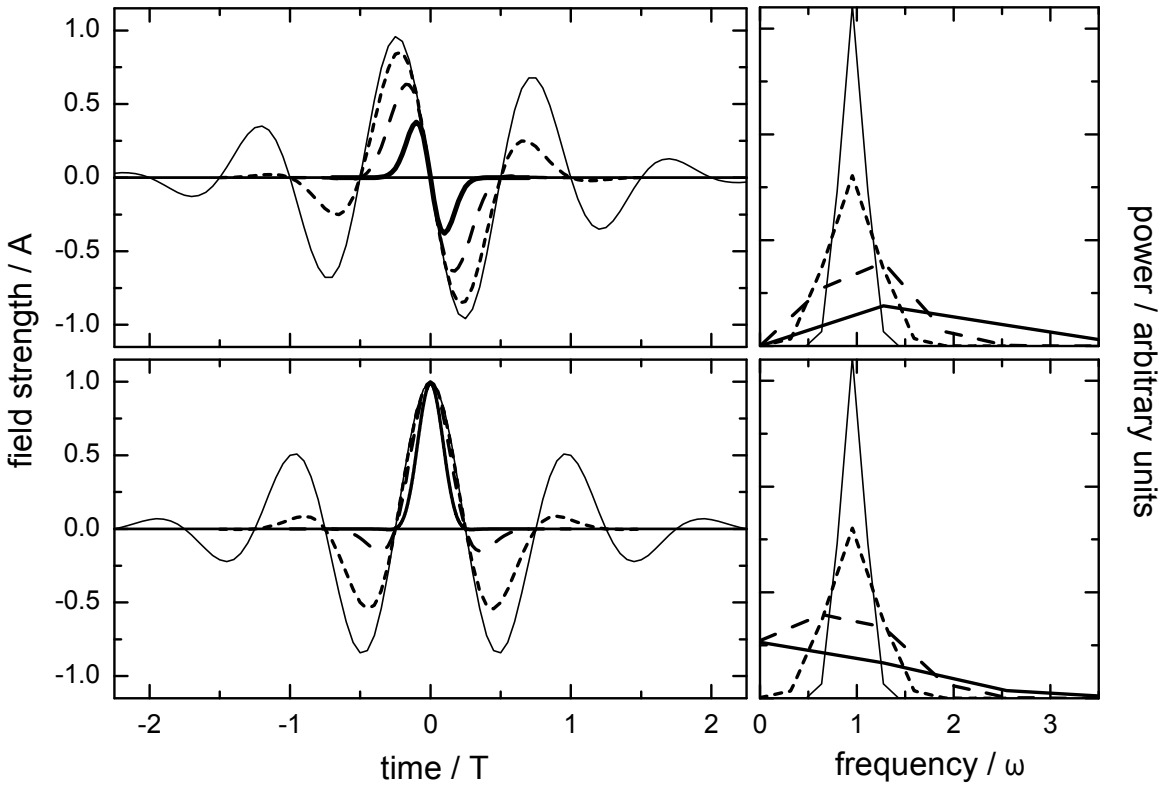
field strength / A
time / T
frequency / ω
power / arbitrary units
1.0
0.5
0.0
-0.5
-1.0
-2
-1
0
1
2
3

FIG. 2:

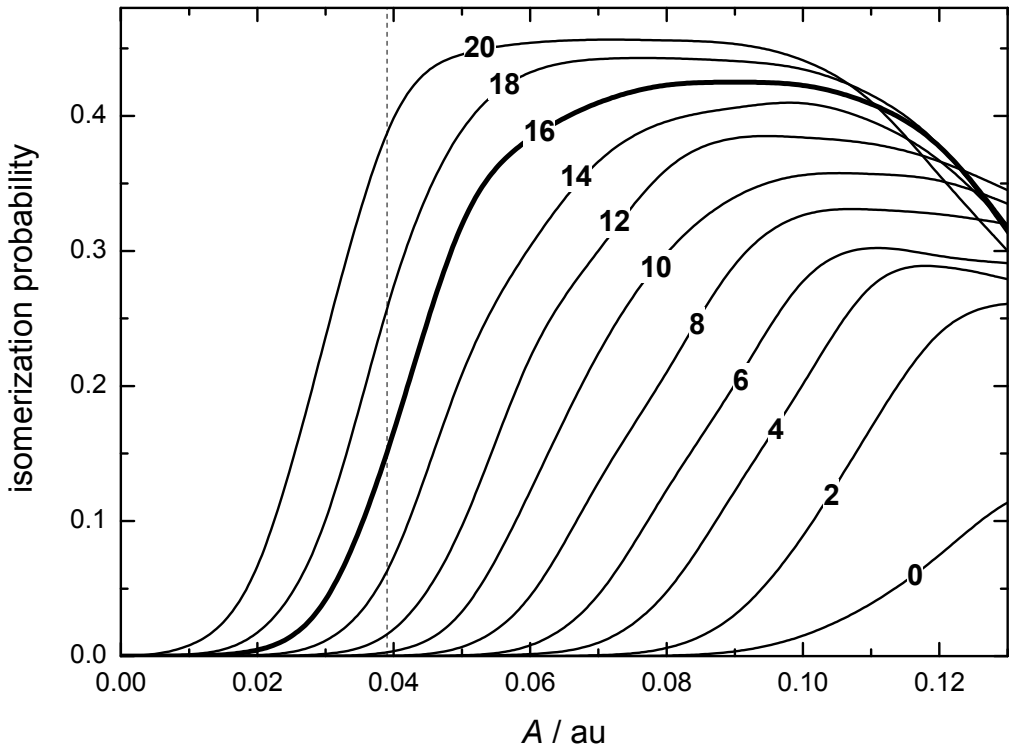
isomerization probability
0.0
0.1
0.2
0.3
0.4
0.00
0.02
0.04
0.06
0.08
0.10
0.12
A / au
20
18
16
14
12
10
8
6
4
2
0

FIG. 3:

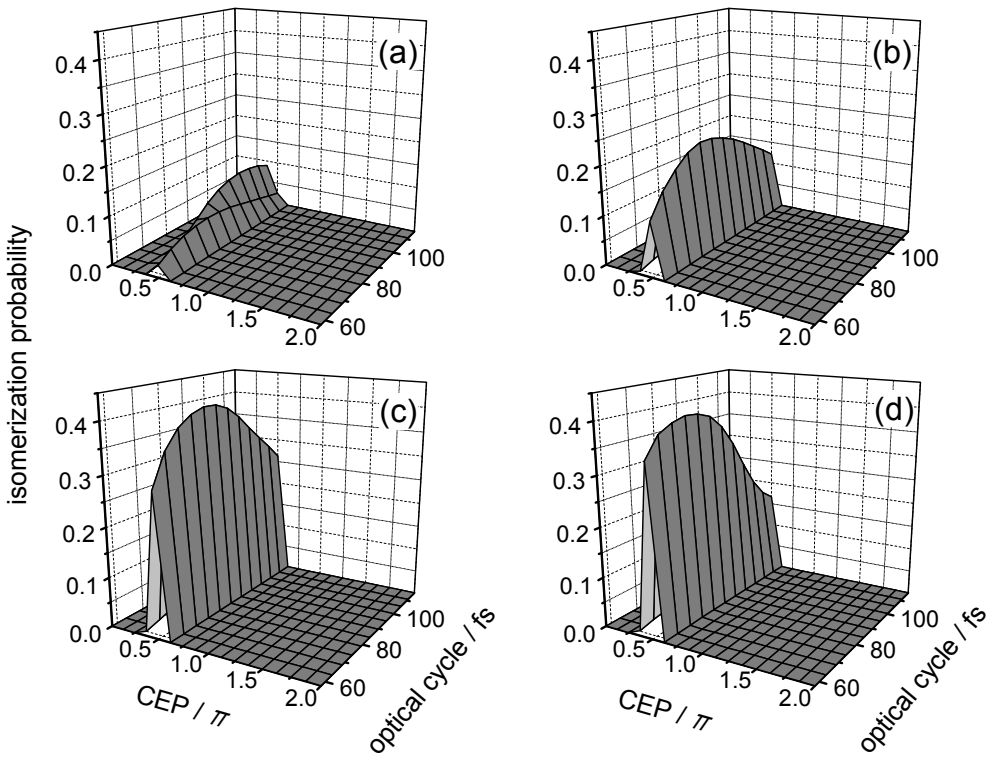
isomerization probability
(a)
(b)
(c)
(d)
0.0
0.1
0.2
0.3
0.4
0.5
1.0
1.5
2.0
CEP / π
60
80
100
optical cycle / fs

FIG. 4:

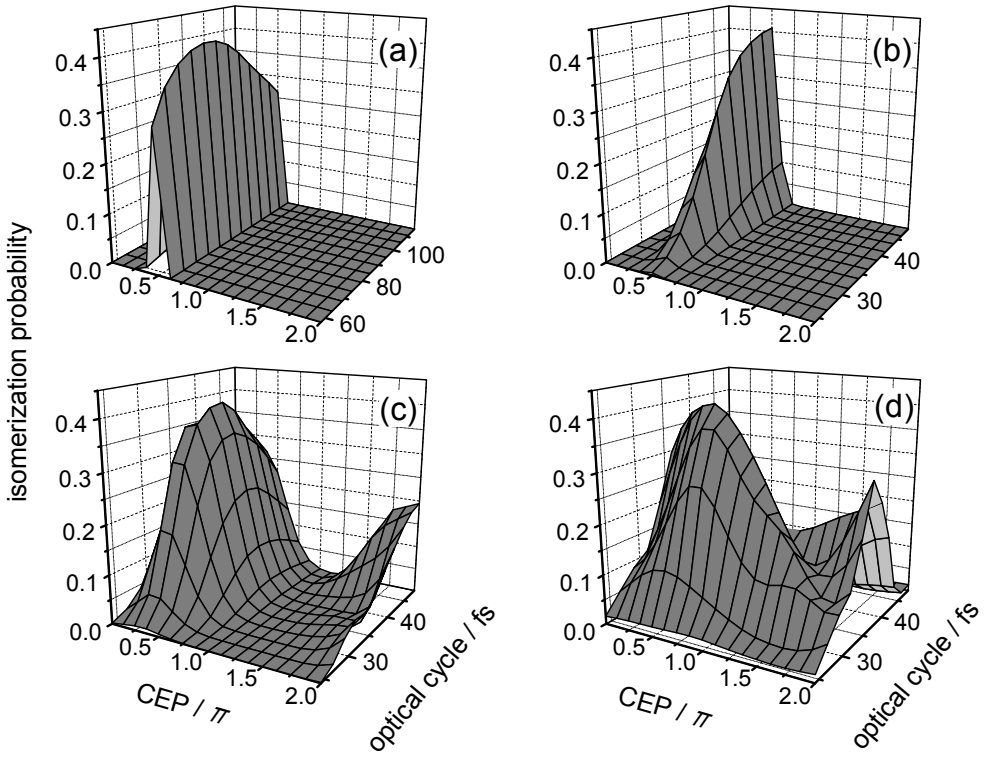
isomerization probability
(a)
(b)
(c)
(d)
0.0
0.1
0.2
0.3
0.4
0.5
1.0
1.5
2.0
CEP / π
60
80
100
30
40
optical cycle / fs

FIG. 5:

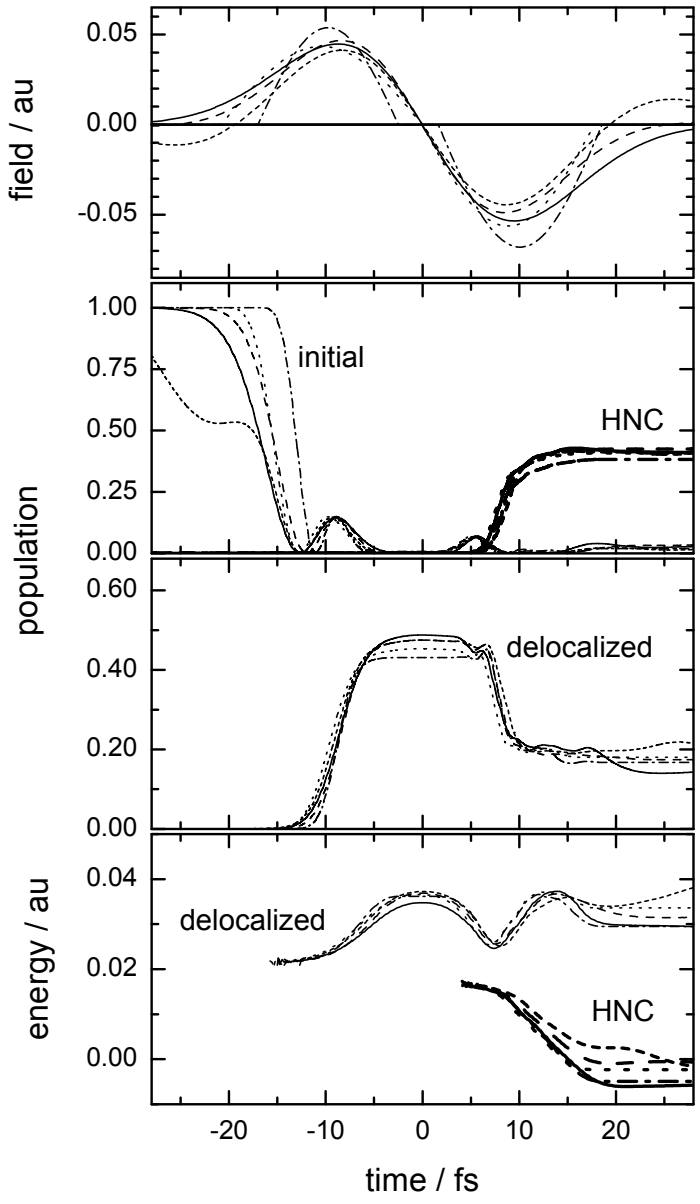
field / au
0.05
0.00
-0.05
population
1.00
0.75
0.50
0.25
0.00
initial
HNC
0.60
0.40
0.20
0.00
delocalized
energy / au
0.04
0.02
0.00
delocalized
HNC
-20
-10
0
10
20
time / fs

FIG. 6:

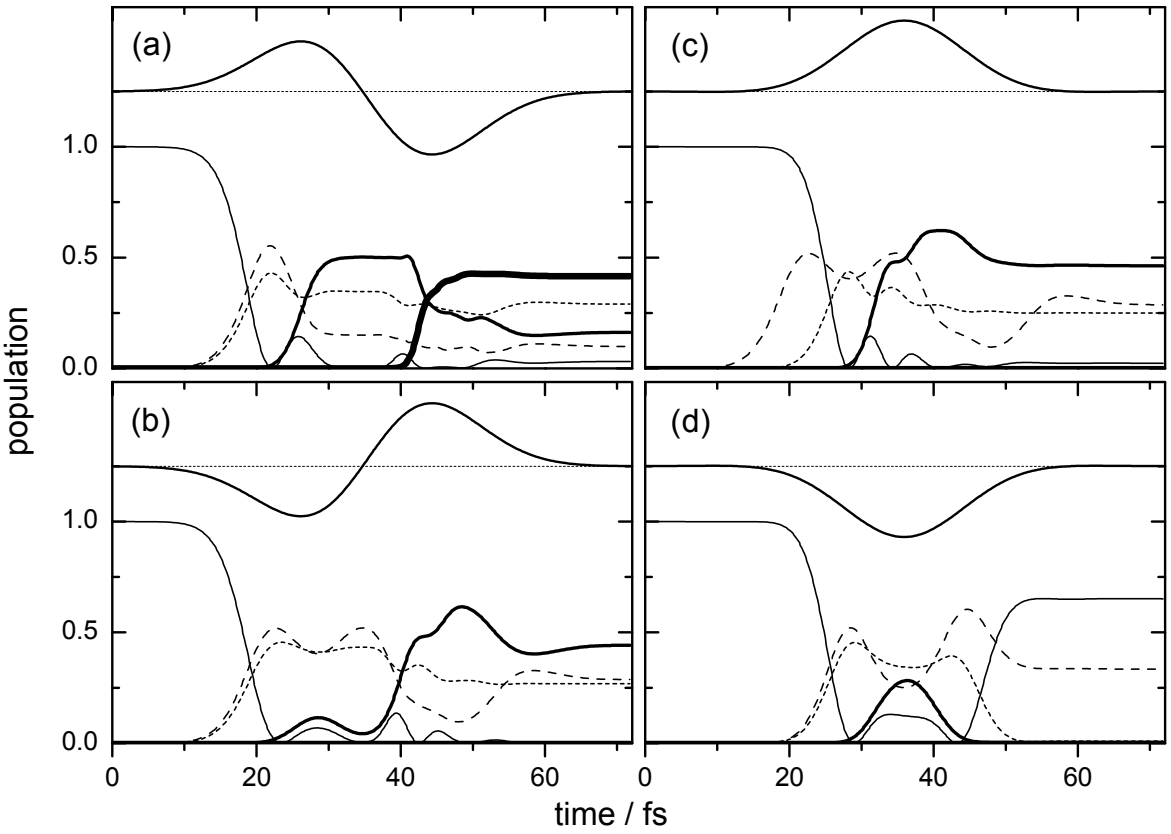

FIG. 7:

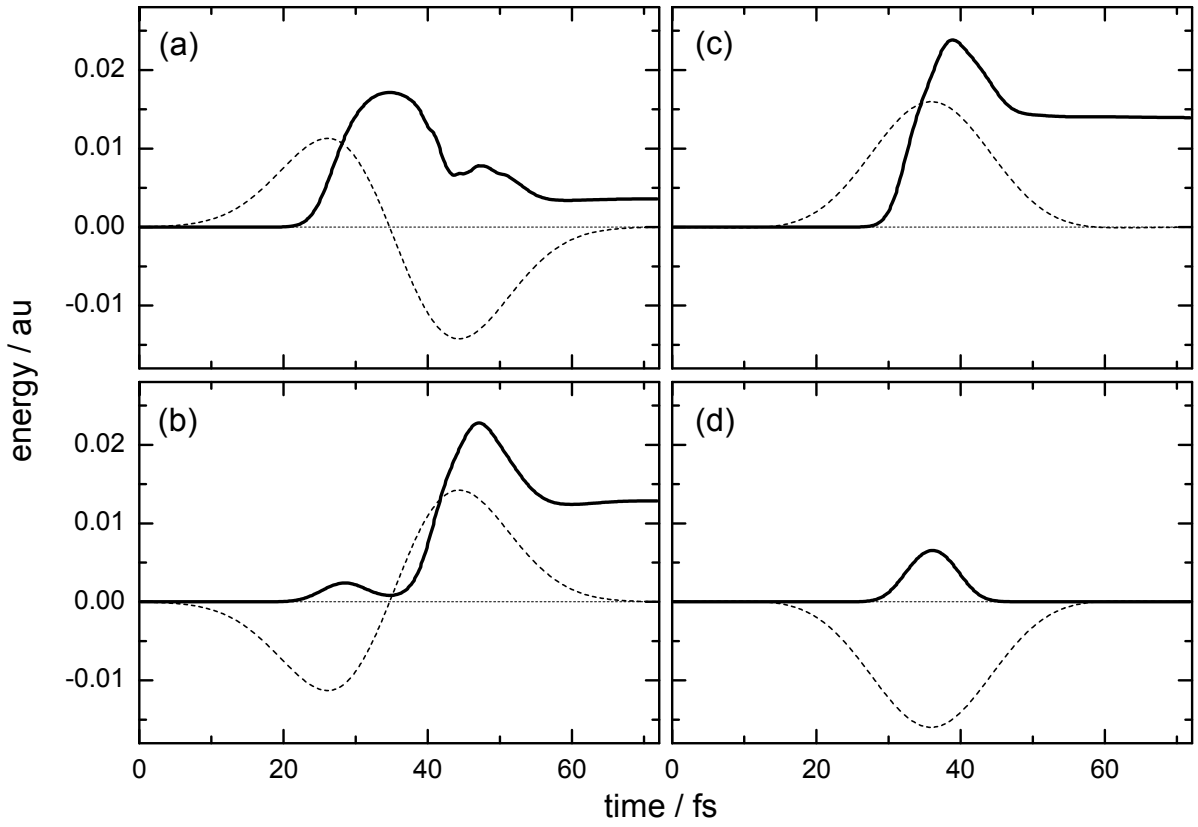

FIG. 8:

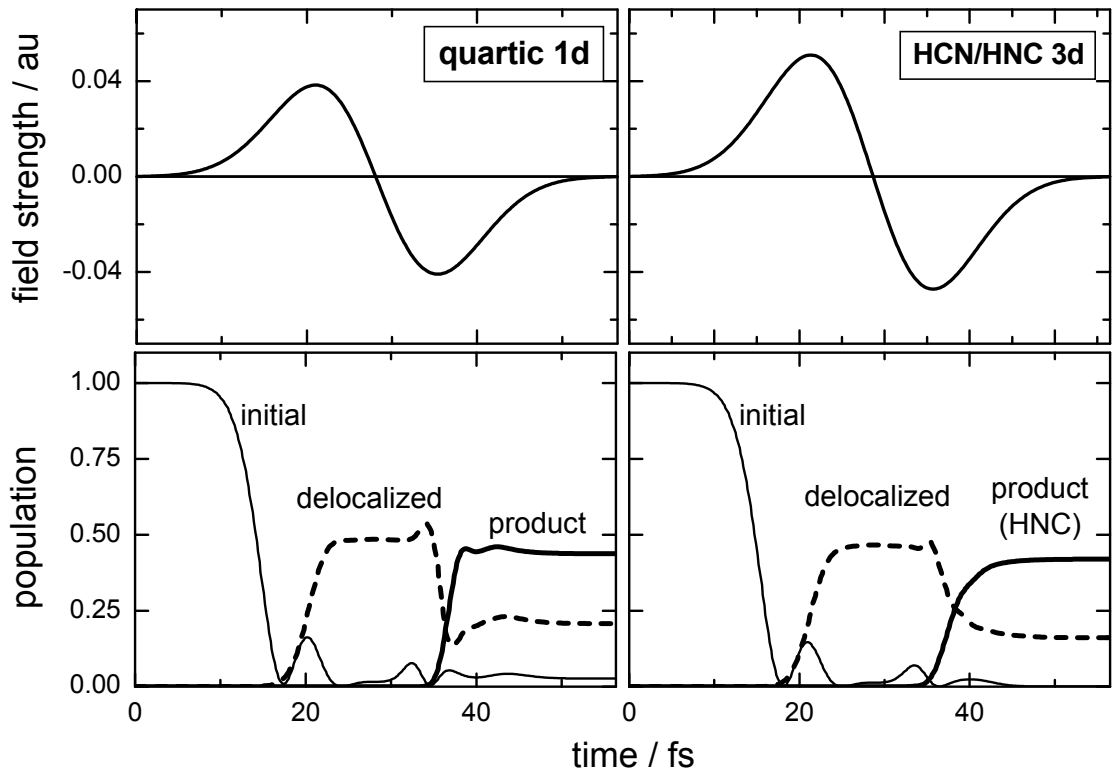
quartic 1d
HCN/HNC 3d
field strength / au
0.04
0.00
-0.04
population
1.00
0.75
0.50
0.25
0.00
initial
delocalized
product
initial
delocalized
product
(HNC)
0
20
40
0
20
40
time / fs

FIG. 9: